Chapter 6

Dielectric relaxation of lithium doped ZnF_2

The work presented in this Chapter has been submitted for publication in Physica B [226].

6.1 Introduction

Many previous studies on alkaline-earth fluoride materials has considered crystals with the cubic symmetry [227–231]. Some studies have also considered materials of lower symmetries, such as tetragonal MnF_2. The reason for studying these non-cubic systems is that the physical properties have a large number of independent relationships resulting from their anisotropic nature [232].

In a study of tetragonal MnF_2 (isostructural to ZnF_2 which is shown in Figure 6.1),

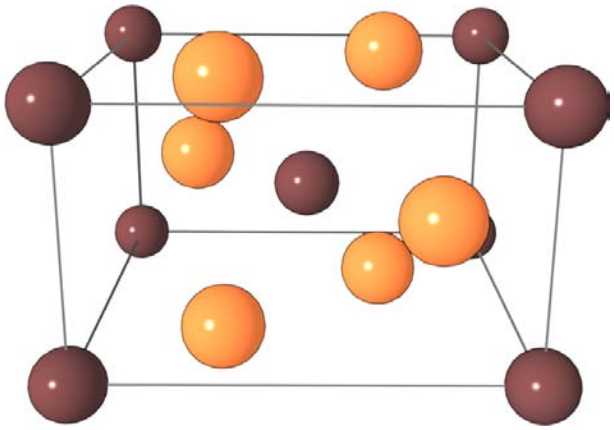

Figure 6.1: The ZnF_2 tetragonal unit cell. The orange spheres represent fluorine ions and the brown spheres represent zinc ions.

Ling *et al.* [232] suggest that the lowest energy intrinsic defect process is anion Frenkel. Studies by Catlow [233] found that the lowest energy intrinsic disorder was indeed anion Frenkel.

Several studies on tetragonal fluoride materials have noticed a split fluorine interstitial defect [232–234]. This is where two fluorine interstitial ions share a lattice site. This split type of defect occurs when an interstitial fluorine ion at an interstitial lattice site displaces a neighbouring fluorine ion from its lattice site towards the next interstitial site leaving behind a fluorine vacancy, as illustrated in Figure 6.2 which shows the orientation of this split defect cluster. Further details in relation to ZnF_2 are given in Section 6.2.

6.1.1 Dielectric Relaxation of lithium doped ZnF_2

Many materials, when subjected to an electric field, will polarize to oppose the field. This polarization can occur via two routes. The first is electronic, with the concerted

motion of the electrons in the direction of the field. The second, and for the purpose of this work most pertinent, is ionic and involves the movement of some ions from their equilibrium lattice positions. When the field is removed, the ions will generally return to their equilibrium positions. If the field is imposed on a material at a high temperature, for some extended time, and the material is subsequently quenched in the field (typically to liquid nitrogen temperature), the ionic contribution to the polarization can be frozen-in to some extent. This implies that there is an energy barrier against the relaxation of the ions back to their equilibrium positions. If the material is slowly heated, this remnant polarization will be lost once the ions gain sufficient thermal energy to overcome the barrier. This process, the dielectric relaxation, can be monitored and quantified as an electric current due to the motion of charged ions [235, 236].

It has been suggested by Roth [237,238] that zinc fluoride (ZnF_2) doped with lithium exhibits a considerable anisotropy in its dielectric properties. In particular, it exhibits a strong relaxation in [001], while the effect in [100] and [110] is several orders of magnitude lower [237]. Several mechanisms for this anisotropic dielectric relaxation have been proposed, the basis of these lies in the initial determination of the defect that charge compensates for the aliovalent Li^+ defect. Roth initially proposed a relaxation mechanism involving the movement of fluorine vacancies, as the charge compensating defects for Li^+ substitutional ions [237] (see Figure 6.3(a)). He later suggested that the anisotropy was due to the motion of Li^+ interstitial ions, as an alternative charge compensating species (see Figure 6.3(b)) [238]. The rationale behind the change in mechanism was an analysis of the experimental data which resulted in a low energy (0.32 eV) for defect cluster reorientation. Roth considered it unlikely that a vacancy model would be responsible for such a low energy but that an interstitial ion model could. The justification was based on previous observations

of low Li^+ interstitial migration energies in materials with the rutile structure [239]. In this regard, Roth suggested that the orientation of the dipole, formed by a "substitutional Li^+ ion - interstitial Li^+ ion" cluster, is initially randomised throughout the lattice with the substitutional lithium defect immobile (see Figure 6.3(b)).

Intriguingly, the anisotropy in the dielectric relaxation was only observed when the doped material was subjected to a prior heat treatment. Again, the reasoning for this treatment differed between the two Roth publications: in the first, it ensures a sufficiently high concentration of fluorine vacancies [237], and in the second it was used to dissolve defect clusters and increase the intensity of the dielectric relaxation [238].

The discrepancies between the two Roth publications was commented on by Nowick [240]. In particular, he stated that the same dielectric response in the [110] and [100] directions is not a test of the relaxation model (as proposed by Roth), but a requirement of the theory. In addition, the experimental data were re-analysed to yield a dipole reorientation energy of about 0.7 eV and as such, the necessity for an interstitial lithium mechanism was removed. Finally Nowick suggested that the dielectric anisotropy could be due merely to differences in the heat treatment of the samples.

It is noteworthy that the anisotropy in the dielectric relaxation in the lithium doped ZnF_2 could also be a result of the tetragonal crystallography of the material as described earlier.

The aim here was to use atomic scale computer simulation to predict the structures and energies of defects associated with lithium solution in ZnF_2. In this way a mechanistic basis for the defect processes that underpin such dielectric relaxation

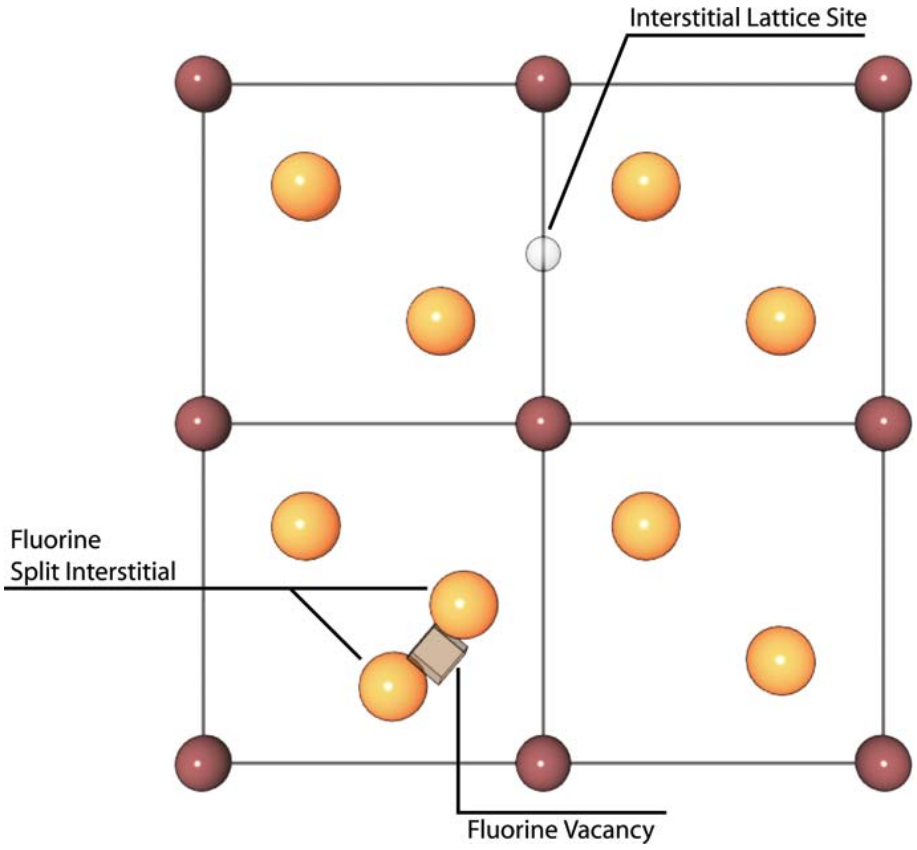

Figure 6.2: Basal plane of ZnF_2 showing the configuration of the split interstitial fluorine cluster.

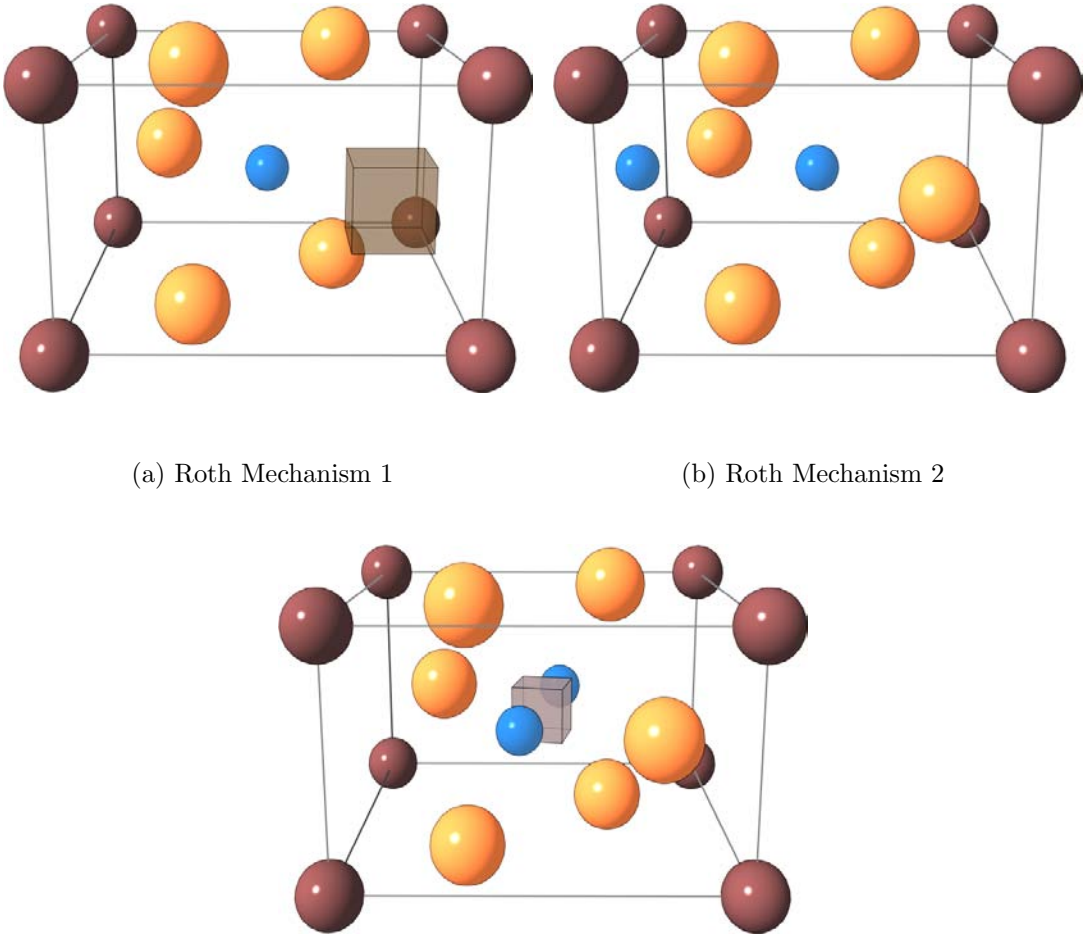

(a) Roth Mechanism 1

(b) Roth Mechanism 2

(c) Levy Mechanism

Figure 6.3: The ZnF_2 tetragonal unit cell showing the three mechanisms discussed in this chapter. a) Represents a schematic of Roth's first proposed mechanism [237], b) represents a schematic of Roth's second mechanism [238], c) represents the mechanism proposed here. The transparent cube in a) represents a fluorine vacancy, the transparent cube in c) is a zinc vacancy and the blue spheres represent lithium substitutional ions in a) and b) but interstitial ions in c).

process in this material will be provided.

6.2 Results for Undoped ZnF_2

ZnF_2 adopts the tetragonal rutile crystal structure with space group 136 ($P4/mnm$). This structure can be considered as a body centered tetragonal lattice of zinc cations which are then octahedrally coordinated by the fluorine anions (see Figure 6.1). The comparison between experimental and calculated lattice parameters, presented in Table 6.1, shows excellent agreement. Elastic constants for ZnF_2 have also been reported experimentally [241–243] and a comparison with values predicted here are presented in Table 6.2. This comparison shows good agreement indicating that displacements of ions around their equilibrium positions are well reproduced.

Table 6.1: Comparison of calculated and experimental lattice parameters for ZnF_2.

	a(Å)	c(Å)	$\frac{c}{a}$	Volume (Å^3)
Calc.	4.6526	3.2046	0.6888	69.37
Expt. [244]	4.7034	3.1335	0.6662	69.32
Percentage Difference	-1.11	2.26	3.41	0.002

Table 6.2: Calculated and experimental elastic constants (x10^{11} Nm^{-2}) for ZnF_2.

	C_{11}	C_{12}	C_{13}	C_{33}	C_{44}	C_{66}
Calc.	131.8	91.4	60.8	214.2	50.1	92.4
Expt. [242, 243]	126	93	84	192	39.2	80.7
Expt. [241]	130	97	89	199	39.5	81.4

Since a lithium doped material is under investigation, the lithium-fluorine potential was derived so that the predicted lattice parameter of LiF, (space group 225 ($Fm\overline{3}m$) [245]) reproduces the experimental data, i.e. a lattice parameter of 4.027 Å.

The energies for intrinsic defect processes in ZnF_2 were also calculated (see Appendix A for details on the normalisation of the defect energies). The results, shown in Table

6.3, suggest that the anion Frenkel reaction is slightly preferred (lower energy) over the Schottky reaction while the cation Frenkel energy is substantially higher. The anion Frenkel defects (i.e. the fluorine vacancy and fluorine interstitial) are therefore the majority intrinsic defects in this material. However, the Schottky reaction is only slightly higher in energy than the anion Frenkel. This reaction will therefore also provide an important concentration of intrinsic defects.

Table 6.3: Normalised, intrinsic defect process energies (eV) for ZnF_2.

Schottky	Anion Frenkel	Cation Frenkel
2.59	2.17	4.31

Finally, when the defects are allowed to cluster, it was found that interstitial F^- adopts a split-interstitial configuration similar to that observed in other fluorite structures [24,233]. In this, the interstitial fluorine ion displaces a lattice F^- ion into a neighbouring interstitial site. Thus, the two F^- ions effectively share the vacant fluorine lattice site that is created. The split-interstitial configuration remains in the ab lattice plane (see Figure 6.2).

6.3 Solution mechanisms for LiF doped ZnF_2

The incorporation of monovalent Li^+ ions onto divalent zinc sites requires charge compensation. This can be facilitated in one of three ways: via a Zn^{2+} interstitial ion (Equation 6.1), a Li^+ interstitial ion (Equation 6.2) or a F^- vacancy (Equation 6.3). Using Kröger-Vink notation [3], these are:

$$2LiF + 2Zn_{Zn}^{X} \rightleftharpoons 2Li'_{Zn} + Zn_i^{\bullet\bullet} + ZnF_2 \tag{6.1}$$

$$2LiF + Zn_{Zn}^{X} \rightleftharpoons Li'_{Zn} + Li_{i}^{\bullet} + ZnF_2 \tag{6.2}$$

$$LiF + Zn_{Zn}^{X} + F_{F}^{X} \rightleftharpoons Li'_{Zn} + V_{F}^{\bullet} + ZnF_2 \tag{6.3}$$

The normalised energies for these processes are reported in Table 6.4 (see Appendix A for details of the normalisation process). It is clear that the energies of these extrinsic defect processes are considerably smaller than those for intrinsic processes. As such, at equilibrium, extrinsic defects will dominate over intrinsic defects.

Initially, it is assumed that the defects remain spatially isolated, and the lowest energy charge compensating defect is a Li^+ interstitial (Equation 6.2). However, Equation 6.3 which describes charge compensation via a F^- vacancy is only 0.19 eV higher, and may on this basis alone yield a further minor, yet significant, concentration of defects.

The coulombic interaction between the isolated defects leads to the formation of defect clusters. The lowest energy solution process, based on defect clusters, still involves compensation via a Li^+ interstitial defect (Equation 6.2). This mechanism is now substantially favoured over the other two reactions (Table 6.4). The reason for this is that the Li^+ interstitial/substitution pair undergoes considerable lattice relaxation when clustering occurs, into a split interstitial configuration, which lowers the overall solution energy. (This is isostructural to the split F^- interstitial ion reported in the intrinsic defect analysis). The structure of this cluster, as shown in Figure 6.3(c), consists of two equivalent Li^+ interstitials either side of a vacant zinc site (i.e. $\{Li_i^{\bullet} : V''_{Zn} : Li_i^{\bullet}\}^X$ rather than $\{Li'_{Zn} : Li_i^{\bullet}\}^X$). This is the referred to as the Levy Mechanism shown in Figure 6.3(c).

Table 6.4: Solution and cluster binding energies (eV) for Li^+ accommodation in ZnF_2.

Solution Mechanism	Charge Compensating Defect	Solution Energy		Cluster Binding Energy
		Isolated*	Clustered	
Reaction 6.1	$Zn_i^{\bullet\bullet}$	2.22	1.82	-4.84
Reaction 6.2	$Li_i^{\bullet}$	1.27	0.73	-1.81
Reaction 6.3	$V_F^{\bullet}$	1.46	1.52	-1.40

* note: these energies have been normalised as described in Appendix A.

Equation 6.4 describes the equilibrium between Li^+ ions when isolated and when part of a defect cluster (indicated by braces).

$$Li'_{Zn} + Li_i^{\bullet} \rightleftharpoons \{Li_i^{\bullet} : V''_{Zn} : Li_i^{\bullet}\}^X \tag{6.4}$$

The corresponding mass action equation is [3];

$$\frac{\left[\{Li_i^{\bullet} : V''_{Zn} : Li_i^{\bullet}\}^X\right]}{[Li'_{Zn}]\,[Li_i^{\bullet}]} = \exp\left(\frac{-\Delta H_b}{kT}\right) \tag{6.5}$$

where ΔH_b is the cluster binding enthalpy, k is the Boltzman constant, T is the absolute temperature and square brackets indicate a concentration. Using the electroneutrality condition between the charged defects (Equation 6.6), Equation 6.5 can be simplified to yield an expression for the ratio of lithium in clusters to that which is isolated (see Equation 6.7).

$$[Li'_{Zn}] = [Li_i^{\bullet}] \tag{6.6}$$

$$\frac{\text{clustered}}{\text{isolated}} = \frac{\left[\{Li_i^{\bullet} : V''_{Zn} : Li_i^{\bullet}\}^X\right]}{2\,[Li'_{Zn}]} \tag{6.7}$$

If the assumption is made that the total lithium concentration is 100 ppm, as stated by Roth in the experimental studies [237], at the heat treatment temperature of 473 K and the calculated cluster binding energy -1.81 eV (Table 6.4), this ratio has the value $3\text{x}10^7$; *ergo*, at equilibrium, Li^+ ions will be in the form of clusters. On the basis of this analysis, the reason for the heat treatment given by Roth in his second paper [238], that is, to dissolve the clusters, is therefore not valid.

It is also possible to use the calculated defect energies to predict an equilibrium solution limit for Li^+ and compare this against the value given by Roth [237]. In this case, it is assumed that defect clusters dominate and Equation 6.2 is re-written in the form:

$$2LiF + Zn_{Zn}^{X} \rightleftharpoons \{Li_i^{\bullet} : V_{Zn}'' : Li_i^{\bullet}\}^{X} + ZnF_2 \tag{6.8}$$

The corresponding reduced mass action equation is;

$$\left[\{Li_i^{\bullet} : V_{Zn}'' : Li_i^{\bullet}\}^{X}\right] = \exp\left(\frac{-\Delta H_{sol}}{kT}\right) \tag{6.9}$$

where $\Delta H_{sol} = 0.73$ eV, which is the cluster solution energy given in Table 6.4. Using Equation 6.9 the equilibrium solution limit at 473 K is 0.01 parts per million (ppm). This is substantially below the 100 ppm Li^+ ion concentration value suggested to be present by Roth [237].

An assumption of the above analysis is that the Li^+ ion content can reach equilibrium. It is therefore necessary to confirm that the kinetics of the Li^+ interstitial defect are sufficiently fast as to allow access to equilibrium or even for defect clustering to occur in a non-equilibrium material. The migration activation energy for an isolated Li^+ interstitial ion to migrate through the ZnF_2 lattice was therefore calculated. The migration energy in the [001] direction was determined to be 0.01 eV (Figure 6.4), whilst in the basal (ab) plane, the lowest migration activation energy in the [110] direction was 0.9 eV. Since there is an equivalent atomic layer rotated by 90° at the mid point in the unit cell (a translation of $\frac{c}{2}$), and thus the migration in <110> is 0.9 eV (Figure 6.5).

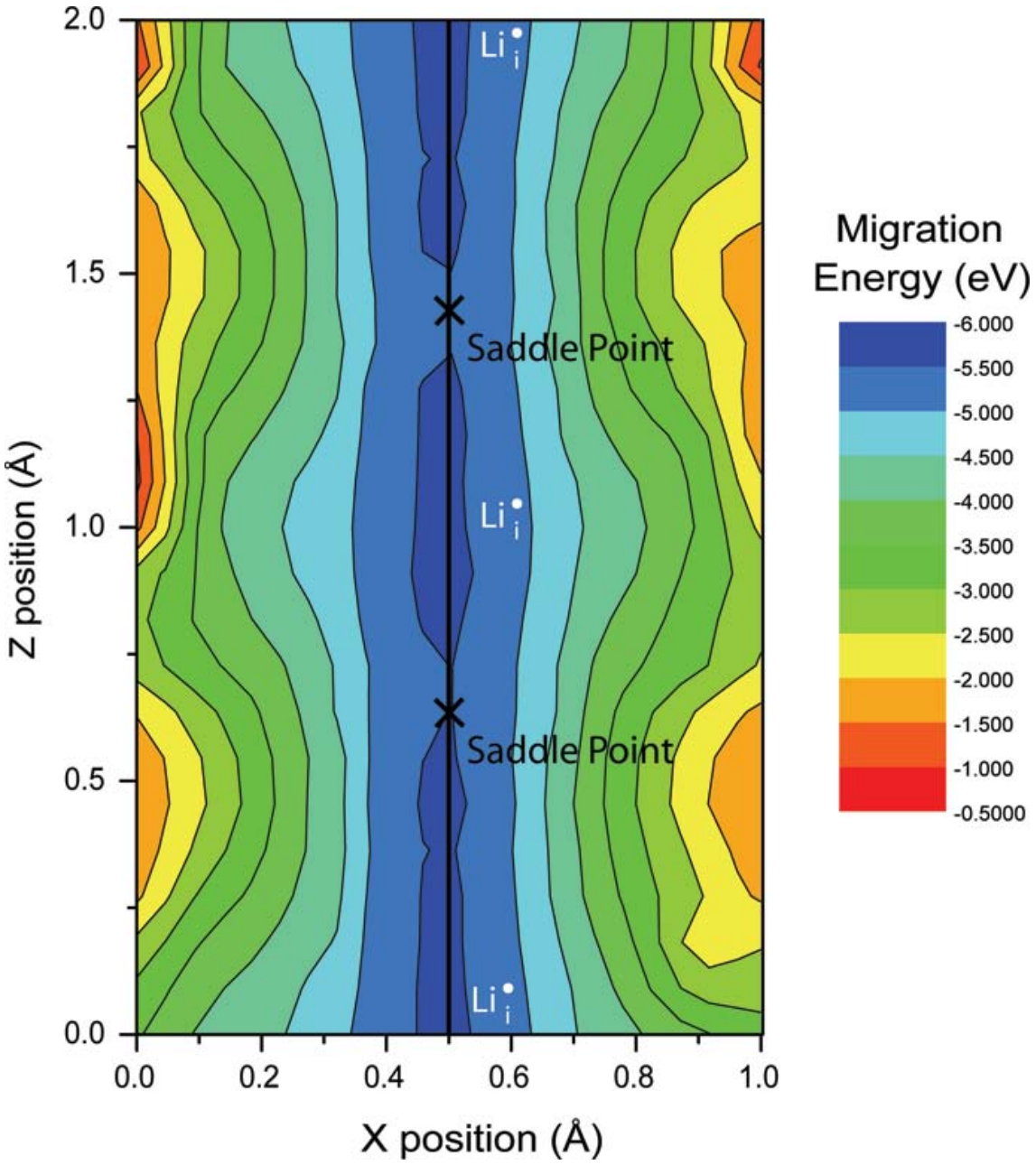

Figure 6.4: Isolated Interstitial Li^+ migration in the [001]. The line indicates the lowest energy pathway.

Since interstitial Li^+ ion migration along [001] is a much lower energy process, it is probable that the isolated Li^+ defects migrate along the [001] until they are either

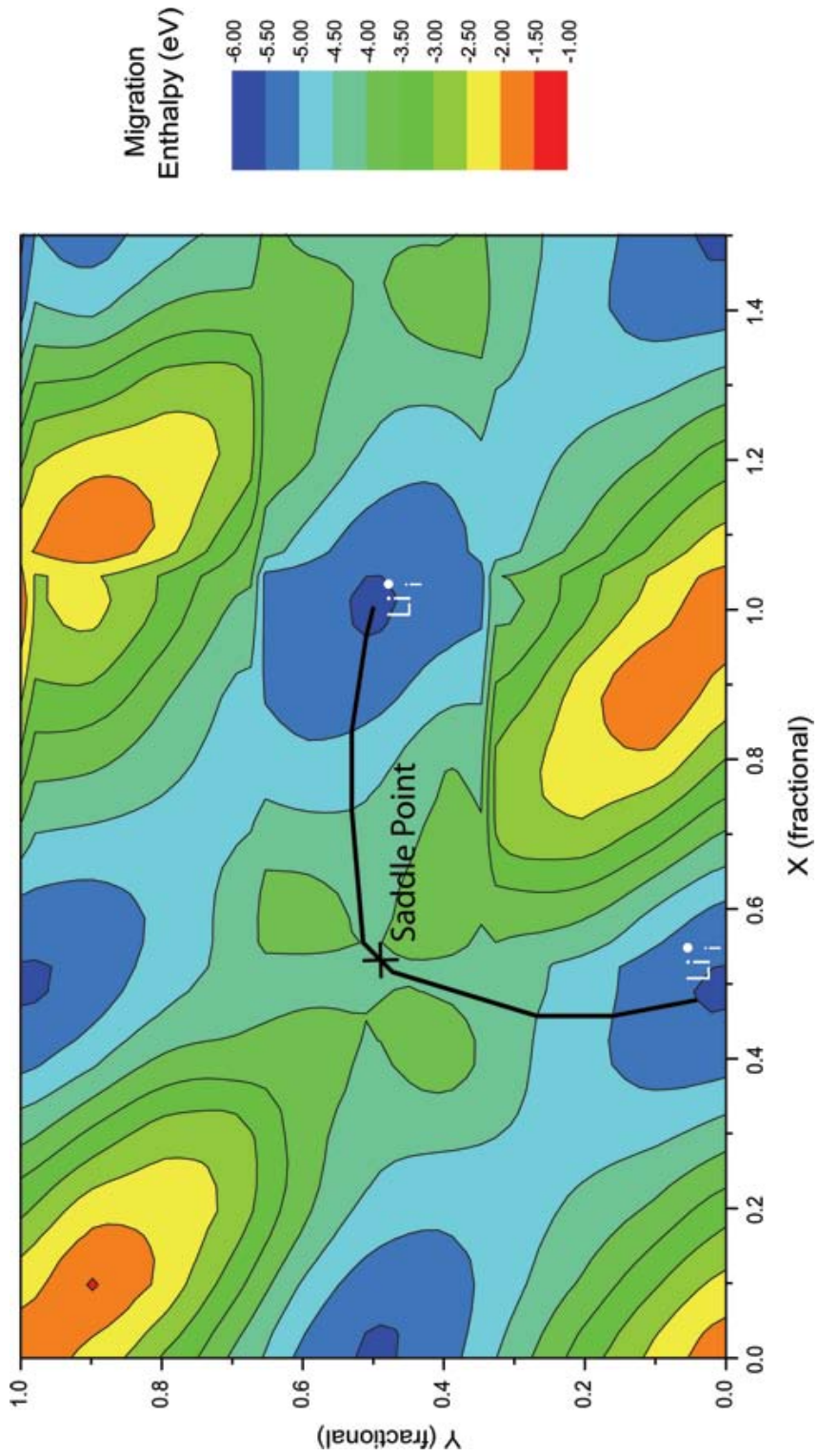

Figure 6.5: Isolated Interstitial Li^+ migration in the ab plane. The line indicates the lowest energy pathway.

trapped in vacant zinc sites, or become part of clusters.

The situation where the Li^+ ion is initially trapped at a zinc site was therefore also considered. In this case, the calculated activation energy is that necessary to move the Li^+ from the substitutional site (leaving behind a vacancy) into a nearest stable interstitial site. If that interstitial site remains in the ab plane, the activation energy is 5.0 eV (the migration energy contour map for this migration is shown in Figure 6.6). If the interstitial migration has a component in the c direction, the activation energy is 3.1 eV (shown in Figure 6.7). In either case, clearly, if the Li^+ defect is trapped at a vacant zinc site, the activation energy is very high.

It is apparent from the earlier analysis that the Li^+ defects take the form of split clusters sharing a vacant zinc lattice site. It therefore follows that there may be some component of the migration that would involve the migration of one of the lithium defects away from this split configuration to a neighbouring interstitial lattice site. This case is shown in Figure 6.8. It is clear that the only migration that is possible is to the 1^{st} interstitial site;, such motion would require an activation energy of 1.5 eV, with migration to a subsequent interstitial sites requiring an additional 2 eV (see Figure 6.8). However, consideration of Table 6.5 shows that when a polarising field is removed, and the lattice is able to respond (relax) to the defect, the split interstitial configuration is adopted once again, i.e. there is effectively no energy barrier for the lattice to relax back to allow the split configuration to reform from a 2^{nd} neighbour split.

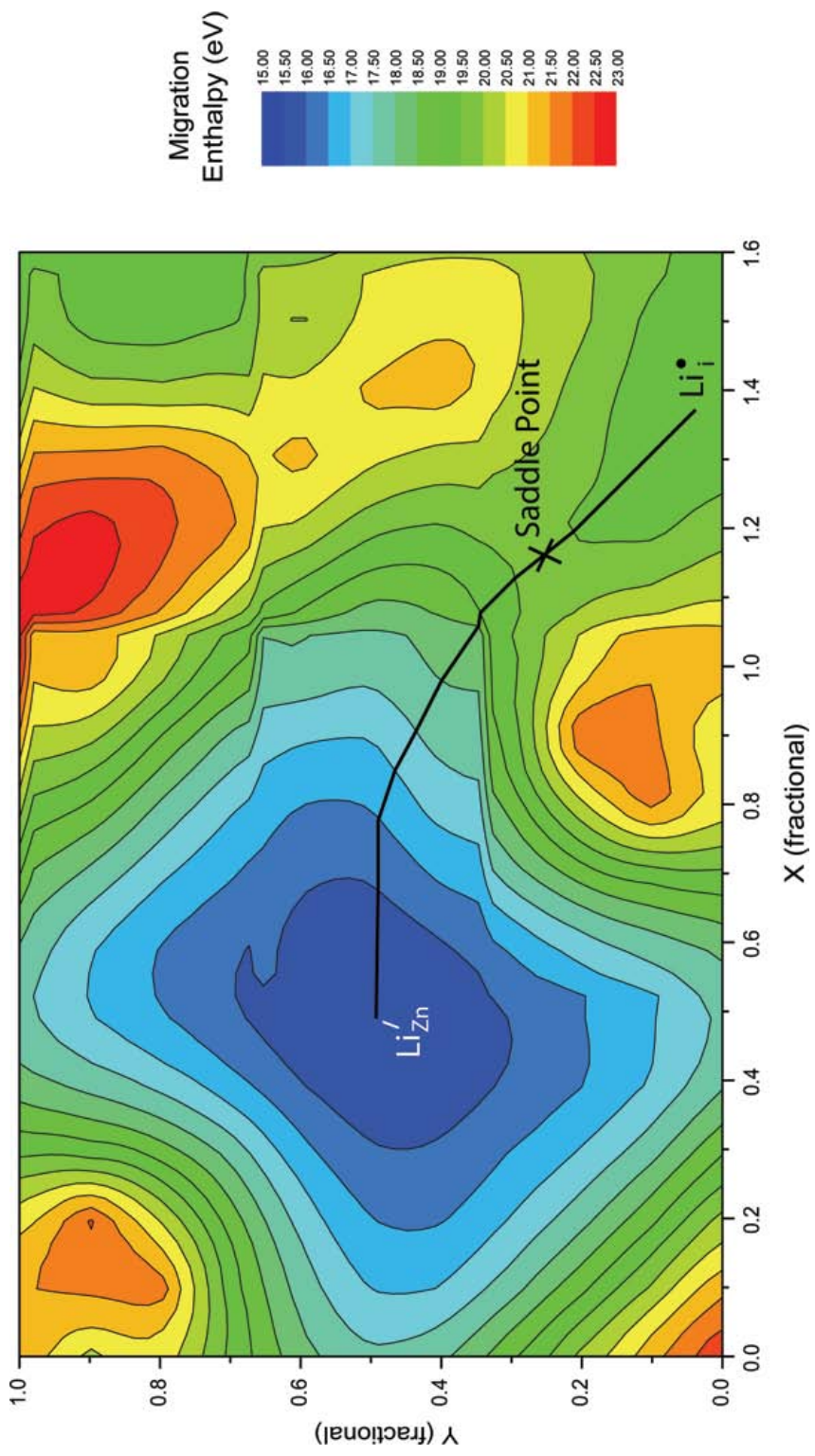

Figure 6.6: Isolated Substitutional Li^+ migration in the ab plane. The line indicates the lowest energy pathway.

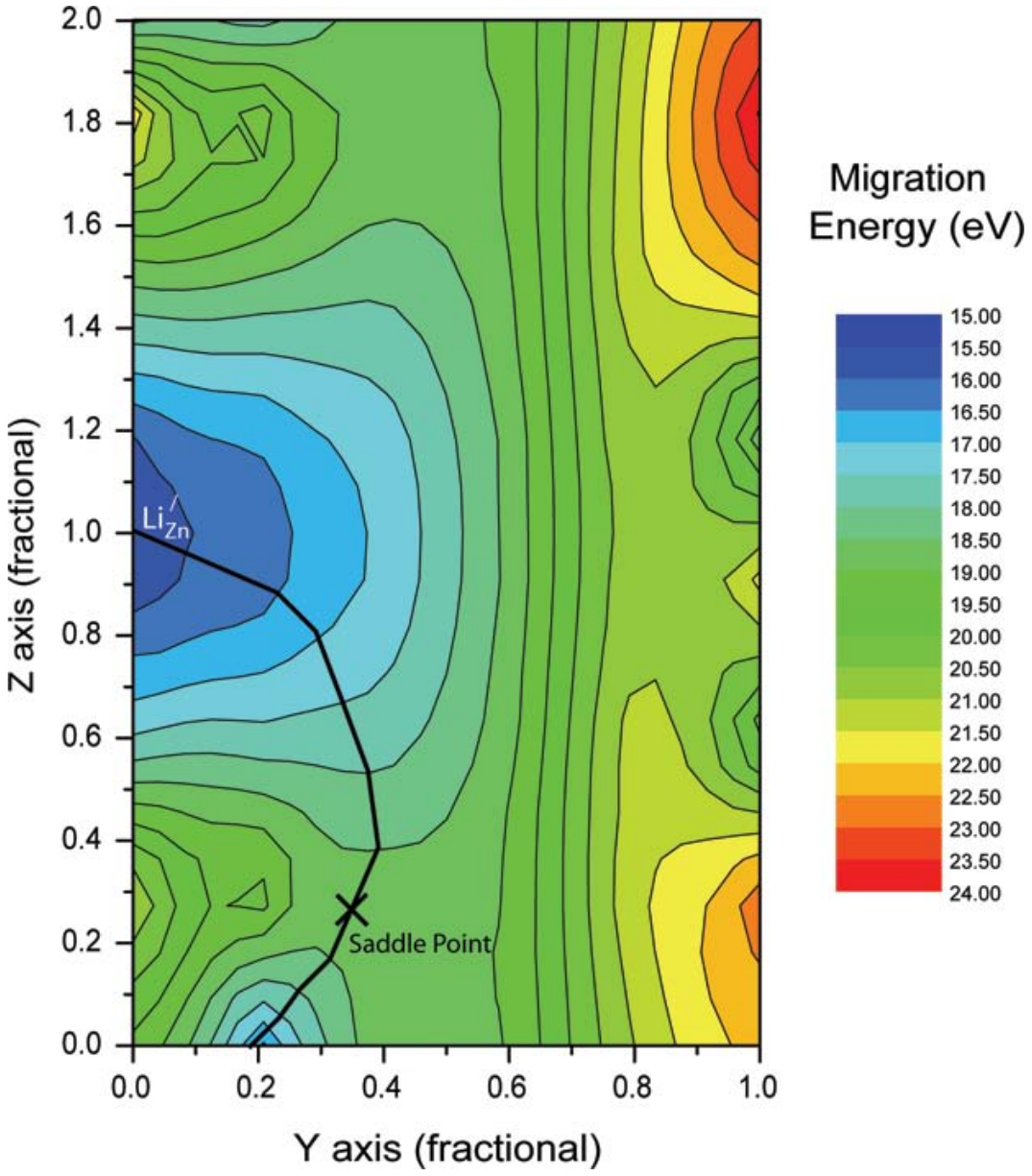

Figure 6.7: Isolated substitutional Li^+ migration in the ac plane. The line indicates the lowest energy pathway.

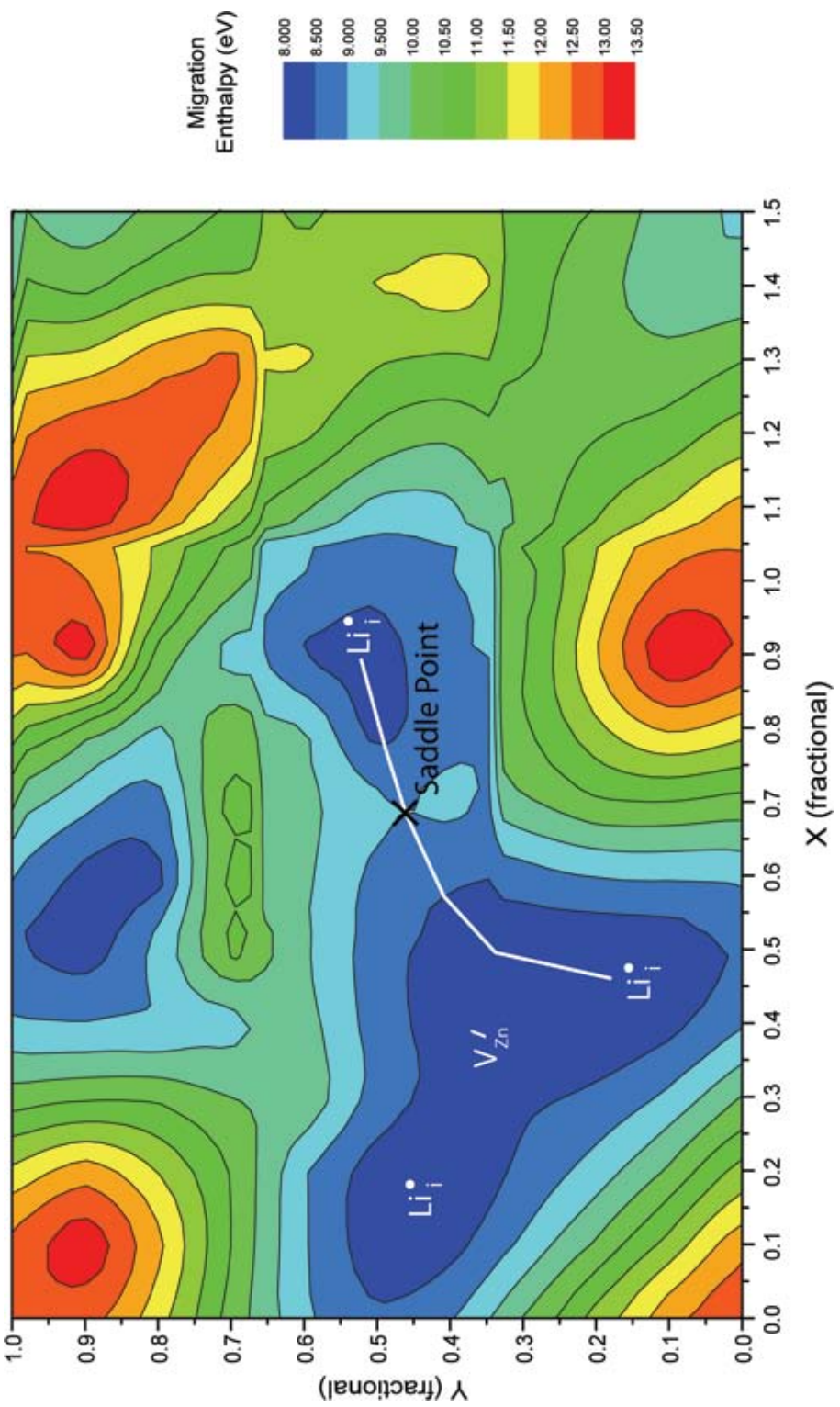

Figure 6.8: Li^+ migration in the ab plane starting from the split defect orientation. The line indicates the lowest energy pathway.

Table 6.5: $\{Li_i^{\bullet} : V_{Zn}'' : Li_i^{\bullet}\}$ cluster energies (eV).

Cluster Neighbour Positions	Relaxation	No Relaxation	Difference
1st	0.73	1.39	0.66
2nd	0.73	1.64	0.91
3rd	1.81	1.85	0.04

6.4 Discussion on the Dielectric Relaxation

Solution energy calculations clearly support the second of Roth's models, i.e. that the dielectric relaxation is governed by lithium interstitial ions. However, the cluster configuration predicted here (Figure 6.3(c)) is quite distinct from the models envisaged by Roth (as shown in Figures 6.3(a) and 6.3(b)). The implications of this to the dielectric relaxation process must now be considered.

First, the way in which this defect cluster couples to an applied field must be investigated. This split lithium cluster is a trimer defect (i.e. +:2-:+) oriented in the [150] direction. As such, if a field is applied parallel to the ab plane, this defect will not couple to the field without reorientation towards the dipole configuration envisaged by Roth (compare Figures 6.3(a) and 6.3(b)). In order to calculate the energies associated with this reorientation, one Li^+ defect is restricted to remain at the substitutional (vacant zinc) site and the Li^+ interstitial is allowed to relax. The calculated energy difference between the two configurations is 0.66 eV (Table 6.5) which is the same as that suggested as the dipole reorientation energy as reanalysed by Nowick [240]. The resulting calculated dipole of the Roth cluster is 7.0×10^{-29} Cm. The problem with this model is, however, when no field is present the defect relaxes back to the split orientation with essentially no energy barrier.

When a field is applied in the [001] direction, the split interstitial defect cluster will

couple with the field and form a dipole most readily by the relaxation of both $Li_i^{\bullet}$ defects in a [001] direction. If the field imparts the same energy (i.e. 0.66 eV) to displace the $Li_i^{\bullet}$ ions, a similar dipole of 2.9x10^{-29} Cm is formed. Once again, when the field is removed, the Li^+ ions will relax back to the $\{Li_i^{\bullet} : V_{Zn}'' : Li_i^{\bullet}\}$ tripole defect with no net polarization of the lattice. Thus, reorientation of the equilibrium defect cluster cannot result in a dielectric relaxation of the type observed by Roth [237,238].

In order to investigate the possible role of the equilibrium lithium cluster in the dielectric relaxation response, the energy of the cluster was considered as a function of defect separation. This was facilitated by placing one Li^+ at a substitutional site and the second Li^+ ion at first, then second and finally third neighbour interstitial sites. Table 6.5 shows the formation energy of the cluster constrained (unrelaxed) and after lattice relaxation. It is immediately clear that when the two Li^+ ions are in either 1st or 2nd neighbour positions (see Figure 6.9) and unconstrained, subsequent energy minimization results in a relaxation to the "split-interstitial" defect orientation. Only, in the 3rd neighbour position do they remain apart; i.e. there is an energy barrier against relaxation to the split interstitial configuration. The resulting 3rd neighbour configuration as shown in Figure 6.9 is oriented in the [203] direction and as such has very similar dipole components both in the ab plane and in the [001] direction. However, the existence of symmetry related equivalent orientations of the 3rd neighbour cluster means that in a purely [001] field, a distribution of such defects can together have a net dipole only in the [001] direction (e.g. [203] + [$\bar{2}$03] and [023] + [0$\bar{2}$3]). Unfortunately, the equivalent holds true for a field applied in the ab plane (e.g. [203] + [02$\bar{3}$] etc.) so it is also possible to construct a dipole response that is restricted to the ab plane.

On the basis of the above analysis, the split Li^+ interstitial cluster cannot be re-

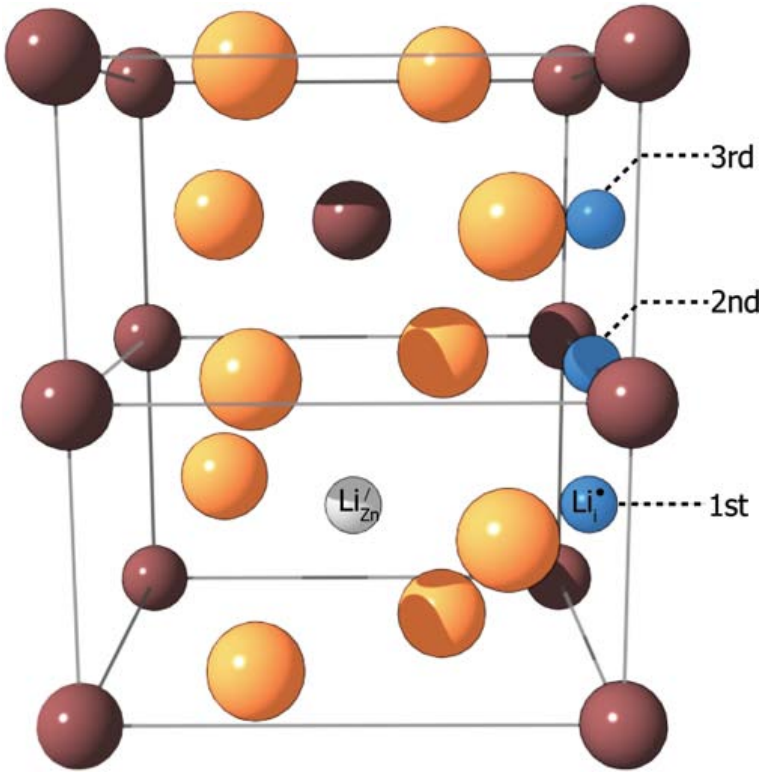

Figure 6.9: The ZnF_2 tetragonal unit cell showing the three different unrelaxed neighbour positions (denoted by the blue spheres) of the Li^+ interstitial defect (1^{st}, 2^{nd}, 3^{rd}) which together with the Li'_{Zn} defect (denoted by the white sphere) will generate the defect cluster $\{Li'_{Zn} : Li_i^{\bullet}\}^x$.

sponsible for the anisotropic dielectric relaxation reported by Roth [237]. However, the earlier solution energy analysis suggests that Roth's material was far from equilibrium. The supersaturated solid solution consisted of essentially immobile substitutional Li^+ ions and charge compensating Li^+ interstitial ions. These later defects are confined to move preferentially in [001] (compare Figures 6.4 and 6.5). Once they encounter a Li^+ substitutional ion they become trapped and form the split Li^+ interstitial cluster. Any untrapped Li^+ interstitial ions will move in [001] subject to an applied field. It is the displacement of these non-equilibrium, residual defects that may conceivably result in a polarization of the crystal. Certainly such a polar-

ization will occur much more strongly in [001] than in the ab plane. Furthermore, the polarization will decay once the temperature is raised to overcome the activation energy barrier. Nevertheless, such defects should eventually become trapped and as such the anisotropic relaxation effects may be subject to a form of thermal cycling fatigue.